Estimation of the Shear Force in Transverse Dynamic Force Microscopy using a Sliding Mode Observer

Thang Nguyen[3], Said G Khan[1], Christopher Edwards[3], Guido Herrmann[1], Loren Picco[2], Robert Harniman[2], Stuart C. Burgess[1], Massimo Antognozzi[2] and Mervyn Miles[2]

Abstract— **This paper concerns the application of a sliding mode observer to the problem of estimation of the shear force affecting the cantilever dynamics of a *Transverse Dynamic Force Microscope* (TDFM). The oscillated cantilever in proximity to a specimen permits the investigation of the specimen topography at nano-metre precision. The oscillation amplitude, but also in particular the shear forces, are a measure of distance to the specimen, and therefore the estimation of the shear force is of significance when attempting to construct TDFM images at submolecular accuracy. For estimation of the shear forces, an approximate model of the cantilever is derived using the method of lines. Model order reduction and sliding mode techniques are employed to reconstruct the unknown shear force affecting the cantilever dynamics based on only tip position measurements. Simulations are presented to illustrate the proposed scheme, which is to be implemented on the TDFM set up at the Centre for NSQI at Bristol.**

I. Introduction

Atomic Force Microscopy (AFM) [1] can produce high resolution images in ambient, aqueous and vacuum environments, making it particularly suited to the study of biological specimens in physiological conditions. The force interaction between the tip of a cantilever and a sample is measured through the induced bending of the cantilever. The force interaction measure, obtained in a raster scan over a sample surface, creates a high resolution topographical image. These devices are typically operated in a contact [1] or intermittent-contact mode [2], [3].

To observe dynamic bio-molecular processes and larger sample areas, a high (sub-second) frame rate is required [4]. Great technological advancements have been made to achieve a higher temporal resolution through improved electronics combined with advanced control approaches [5], [6], via stable fast scan sample stages together with new control approaches [7] and through miniaturisation of cantilevers [8]. Miniaturisation of cantilevers of a given material dramatically increases their resonance frequency and increases the bandwidth of the detection system [9]. The dimensions of AFM cantilevers have been reduced to almost the optical limit of the AFM detection system [4].

The *Transverse Dynamic Force Microscope* (TDFM) addresses the issue of non-contact imaging from a different angle (see Figure 1): The vertically oriented cantilever (VOC) is horizontally, sinusoidally oscillated by a piezo actuator close to its fundamental flexural mode, typically with an amplitude of less than 1 nm. As the tip is lowered via a z-actuation system towards the surface, a shear force interaction produces a reduction in the oscillation amplitude, measured on the photo-detector. Thus, the short-range (less than 2 nm) lateral force between a vertically oriented cantilever (VOC) and a surface is measured by recording changes in the cantilever resonant dynamics. It has been shown that when the TDFM operates in ambient conditions, the visco-elastic response of the water layer between the tip and the surface is responsible for the contrast mechanism [10]–[12]. The vertical orientation of the cantilever in the TDFM prevents the "snap-to-contact" experienced by conventional AFM cantilevers when the gradient of the surface attractive force becomes larger than the spring constant of the cantilever [13]. The combination of VOCs with a scattered evanescent wave (SEW) detection system [14] (Figure 1, items A, B and photo-diode) provides increased TDFM scan rates [15]. The high resolution of the SEW system allows miniaturisation of VOCs far beyond those of standard AFM cantilevers, providing a higher force sensitivity [16]. The SEW feedback enables the user to control the vertical position of the tip with less than a nano meter accuracy.

From the arguments above, the micro cantilever probe in the TDFM (and in AFMs in general) is the most vital part of an atomic force microscope. The dynamic changes occurring in the cantilever probe while interacting with the bio-specimen carry a wealth of information related to the bio-specimen topography and mechanical characteristics. Hence, it is very important to understand the dynamic behaviour of the cantilever scanning probe and identify its key model parameters. The problem of estimation of the cantilever parameters in AFM devices has been investigated for many years. Besancon *et al.* considered an observer-based approach to estimate some unknown force affecting the dynamics of a cantilever in *Electric Force Microscopy* devices [17]. Xu *et al.* studied a two degree of freedom mathematical model of a tapping mode AFM when the cantilever is immersed in liquid, from which the tip-sample interaction forces are extracted [18]. In contrast to much of the AFM research literature (which uses horizontally oriented cantilever), we investigate the problem of estimating the tip-sample interaction forces in the TDFM, which employs a non-contact scanning regime and the cantilever probe has vertical orientation.

[1] Department of Mechanical Engineering, University of Bristol, University Walk, Bristol, BS8 1TR, UK; Corresponding Author at Bristol: G.Herrmann@bris.ac.uk

[2] Centre for Nanoscience and Quantum Information, University of Bristol, Tyndall Avenue, Bristol, BS8 1FD, UK

[3] College of Engineering, Mathematics and Physical Sciences, University of Exeter, Exeter UK EX4 4QF, UK; Corresponding Author at Exeter: C.Edwards@exeter.ac.uk

It is well established that sliding mode observers exhibit a high degree of accuracy in estimating state variables and unknown inputs, see [19]–[23] and the references therein. For this reason, various problems in fault detection and isolation can also be addressed using sliding mode observers, which can detect or reconstruct parameters such as state variables, faults or unknown inputs, from the available information from the system under consideration [24]–[26]. In this paper, an observer will be designed based on the method presented in [19], where the equivalent output injection signal is exploited to accurately reconstruct the unknown tip-sample shear force, which results from the interaction of the cantilever with the ordered liquid layers just above the specimen.

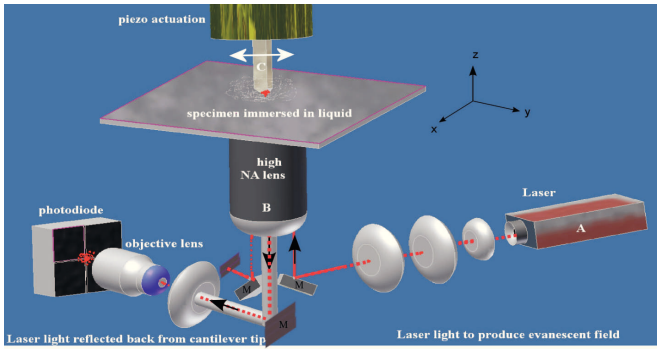

Fig. 1. Simplified schematic of the TDFM together with SEW system (adopted from [15]).

There are two main contributions in this research work. Firstly, it proposes an ordinary differential equation (ODE) model for the dynamics of the vertically installed cantilever (fully immersed in liquid) of the TDFM. Secondly, a sliding mode technique is introduced to estimate the tip-sample interaction force, which is novel in terms of its realm of application. Understanding the dynamics of the TDFM cantilever probe is also an important pre-requisite for high speed control at nano-precision.

A. Problem formulation

To model the cantilever shear force interaction [27], the spatio-temporal dynamics of the cantilever with shear force are best presented in the following equation

$$\frac{\partial^4 EI(Y+\alpha\dot{Y})}{\partial\zeta^4} + \rho A_s \ddot{Y} + \gamma w \dot{Y} = 0 \tag{1}$$

with boundary conditions

$$Y(\zeta=0) = u(t) = d_0\sin(\omega t), \tag{2}$$

$$\frac{\partial Y}{\partial\zeta}(\zeta=0) = 0, \tag{3}$$

$$\frac{\partial^2 Y}{\partial\zeta^2}(\zeta=L) = 0, \tag{4}$$

$$EI\frac{\partial^3 Y}{\partial\zeta^3}(\zeta=L) = -f(t), \tag{5}$$

where E is the Young's modulus, α is the internal damping constant of the cantilever, I is the second moment of area, A_s is the cross-sectional area, ρ is the density of the probe, γ is the damping coefficient of the surrounding fluid, L is the length of the cantilever, w is the width of the cantilever, ζ denotes position along the probe axis, Y is the transversal displacement at any point along the probe during vibration, $\dot{Y}$ and $\ddot{Y}$ are the first and second derivatives of Y with respect to time t, $u(t)$ is the harmonic excitation signal with frequency ω and amplitude d_0 applied at the top of the cantilever, and finally $f(t)$ is the tip-sample interaction force applied at the tip of the cantilever. Furthermore the tip sample interaction force applied at the tip can be split into a viscous and an elastic force [28]:

$$f(t) = -\nu\frac{\partial Y}{\partial t}\bigg|_{\zeta=L} - \kappa Y(L) \tag{6}$$

where ν is the dissipative interaction constant and κ is the elastic interaction constant. Our aim in this paper is to estimate the unknown shear force signal $f(t)$, which will allow better interpretation and understanding of the scan result.

II. Main Results

In this section, we will introduce the method of lines to approximate the partial differential equation (PDE) (1) by a system of linear time-invariant (LTI) ordinary differential equations (ODEs) [29].[1] Subsequently, a reduced-order model will be obtained by balanced truncation [30] of the LTI. A sliding mode observer will be presented to reconstruct the tip-sample interaction shear force.

A. Modelling of the cantilever using the method of lines

The idea is to divide the probe into $n-1$ equal sections and to consider n nodes distributed along the probe. Denote Y_j as the displacement at node j and $\delta\zeta$ as the distance between two consecutive nodes. Using finite difference formula the boundary condition (3) for the approximate model becomes

$$\frac{\partial Y}{\partial\zeta}(\zeta=0) \approx \frac{Y_2 - Y_1}{\delta\zeta} = 0 \tag{7}$$

which implies

$$Y_2 = Y_1. \tag{8}$$

The boundary conditions in (4) becomes

$$\frac{\partial^2 Y}{\partial\zeta^2}(\zeta=L) \approx \frac{Y_n - 2Y_{n-1} + Y_{n-2}}{\delta\zeta^2} = 0 \tag{9}$$

or equivalently

$$Y_n - 2Y_{n-1} + Y_{n-2} = 0. \tag{10}$$

Finally (5) can be approximated as

$$EI\frac{\partial^3 Y}{\partial\zeta^3}(\zeta=L) \approx EI_n\frac{Y_n - 3Y_{n-1} + 3Y_{n-2} - Y_{n-3}}{\delta\zeta^3} = -f(t) \tag{11}$$

[1]This approach also retains some of the versatility of the PDE, as forces and the level of ambient fluid can be modeled with good accuracy by choosing for instance the model parameter γ as function of ζ. In our case, the cantilever is fully immersed in fluid, and homogeneous values for γ will be used.

From (2), (8), (10) and (11) it is clear that the values of Y_1, Y_2, Y_n, and Y_{n-1} are 'known', i.e dependent on the dynamics of the remaining nodes. Hence, we only need to understand the dynamics of $n-4$ nodes. Each of these nodes is described by a second-order ODE. Hence, the dynamics of the cantilever can be represented by a state space system of order of $2(n-4)$.

The fourth partial derivative of Y with respect to the spatial variable ζ in the PDE can be approximated as follows

$$\frac{\partial^4 Y_j}{\partial \zeta^4} \approx \frac{Y_{j+2} - 4Y_{j+1} + 6Y_j - 4Y_{j-1} + Y_{j-2}}{\delta\zeta^4} \tag{12}$$

for $j = 3, ..., n-3$. From the boundary conditions for the approximate model, the dynamics of nodes Y_3, Y_4 are given by

$$\begin{aligned}\ddot{Y}_3 =&\frac{1}{\rho A_3}\left(-(\frac{6\alpha EI_3}{\delta\zeta^4} + \gamma_3 w_3)\dot{Y}_3 - \frac{6EI_3}{\delta\zeta^4}Y_3 + \frac{4EI_3}{\delta\zeta^4}(Y_4\right.\\ &\left. + \alpha\dot{Y}_4) - \frac{EI_3}{\delta\zeta^4}(Y_5 + \alpha\dot{Y}_5) + \frac{3EI_3}{\delta\zeta^4}(u + \alpha\dot{u})\right), \end{aligned}\tag{13}$$

$$\begin{aligned}\ddot{Y}_4 =&\frac{1}{\rho A_4}\left(-(\frac{6\alpha EI_4}{\delta\zeta^4} + \gamma_4 w_4)\dot{Y}_4 - \frac{6EI_4}{\delta\zeta^4}Y_4 + \right.\\ &+ \frac{4EI_4}{\delta\zeta^4}(Y_3 + \alpha\dot{Y}_3) + \frac{4EI_4}{\delta\zeta^4}(Y_5 + \alpha\dot{Y}_5)\\ &\left. - \frac{EI_4}{\delta\zeta^4}(Y_6 + \alpha\dot{Y}_6) - \frac{EI_4}{\delta\zeta^4}(u + \alpha\dot{u})\right), \end{aligned}\tag{14}$$

From (8) and (10), we have

$$Y_{n-1} = 2Y_{n-2} - Y_{n-3} + \frac{\delta\zeta^3}{EI_n}f \tag{15}$$

$$Y_n = 3Y_{n-2} - 2Y_{n-3} + 2\frac{\delta\zeta^3}{EI_n}f \tag{16}$$

For node $j = n-3$, we have

$$\begin{aligned}\frac{\partial^4 Y_{n-3}}{\partial\zeta^4} \approx&\frac{1}{\delta\zeta^4}\left(-2Y_{n-2} + 5Y_{n-3} - 4Y_{n-4} + Y_{n-5}\right.\\ &\left. + \frac{\delta\zeta^3}{EI_n}f\right). \end{aligned}\tag{17}$$

As a result, the dynamics of Y_{n-3} are given by

$$\begin{aligned}\ddot{Y}_{n-3} =& \frac{1}{\rho A_{n-3}}\left(-(\frac{5\alpha EI_{n-3}}{\delta\zeta^4} + \gamma_{n-3}w_{n-3})\dot{Y}_{n-3}\right.\\ &- \frac{5EI_{n-3}}{\delta\zeta^4}Y_{n-3} + \frac{4EI_{n-3}}{\delta\zeta^4}(Y_{n-4} + \alpha\dot{Y}_{n-4})\\ &- \frac{EI_{n-3}}{\delta\zeta^4}(Y_{n-5} + \alpha\dot{Y}_{n-5}) + \frac{2EI_{n-3}}{\delta\zeta^4}(Y_{n-2} + \alpha\dot{Y}_{n-2})\\ &\left. - \frac{I_{n-3}}{\delta\zeta I_n}(f + \alpha\dot{f})\right), \end{aligned}\tag{18}$$

Similarly for node $j = n-2$, we have

$$\frac{\partial^4 Y_{n-2}}{\partial\zeta^4} \approx \frac{1}{\delta\zeta^4}\left(Y_{n-2} - 2Y_{n-3} + Y_{n-4} - 2\frac{\delta\zeta^3}{EI_n}f\right).$$

Thus, the dynamics of Y_{n-2} are described as

$$\begin{aligned}\ddot{Y}_{n-2} =& \frac{1}{\rho A_{n-2}}\left(-(\frac{\alpha EI_{n-2}}{\delta\zeta^4} + \gamma_{n-2}w_{n-2})\dot{Y}_{n-2}\right.\\ &- \frac{EI_{n-2}}{\delta\zeta^4}Y_{n-2} + \frac{2EI_{n-2}}{\delta\zeta^4}(Y_{n-3} + \alpha\dot{Y}_{n-3}) -\\ &\left.\frac{EI_{n-2}}{\delta\zeta^4}(Y_{n-4} + \alpha\dot{Y}_{n-4}) + \frac{2I_{n-2}}{\delta\zeta I_n}(f + \alpha\dot{f})\right), \end{aligned}\tag{19}$$

An ODE for node j $(j = 5, ..., n-4)$ is given by

$$\begin{aligned}\ddot{Y}_j =&\frac{1}{\rho A_j}\left(-(\frac{6\alpha EI_j}{\delta\zeta^4} + \gamma_j wj)\dot{Y}_j - \frac{6EI_j}{\delta\zeta^4}Y_j\right.\\ &- \frac{EI_j}{\delta\zeta^4}(Y_{j-2} + \alpha\dot{Y}_{j-2} + Y_{j+2} + \alpha\dot{Y}_{j+2})\\ &\left. + \frac{4EI_j}{\delta\zeta^4}(Y_{j-1} + \alpha\dot{Y}_{j-1} + Y_{j+1} + \alpha\dot{Y}_{j+1})\right). \end{aligned}\tag{20}$$

Denote the state variables as follows

$$\begin{aligned} x_1 &= Y_3, & x_2 &= \dot{Y}_3 - \frac{3EI_3}{\rho A_3\delta\zeta^4}\alpha u,\\ x_3 &= Y_4, & x_4 &= \dot{Y}_4 + \frac{EI_4}{\rho A_4\delta\zeta^4}\alpha u,\\ x_{2n-11} &= Y_{n-3}, & x_{2n-10} &= \dot{Y}_{n-3} + \frac{I_{n-3}}{\rho A_{n-3}\delta\zeta I_n}\alpha f,\\ x_{2n-9} &= Y_{n-2}, & x_{2n-8} &= \dot{Y}_{n-2} - \frac{2I_{n-2}}{\rho A_{n-2}\delta\zeta I_n}\alpha f, \end{aligned}$$

and $x_{2j-5} = Y_j,\ x_{2j-4} = \dot{Y}_j$ for $j = 5, ..., n-4$. Then, by construction the LTI system

$$\dot{x}_p = A_p x_p + B_p u + D_p f \tag{21}$$

$$y = C_p x_p \tag{22}$$

where $A_p \in \mathbb{R}^{2(n-4)\times 2(n-4)}$, $B_p \in \mathbb{R}^{2(n-4)\times 1}$ and $D_p \in \mathbb{R}^{2(n-4)\times 1}$ is a good approximation of the PDE assuming $\delta\zeta$ is small enough. In the above, the output y is taken as Y_{n-2} and hence the $(2n-9)th$ entry of $C_p \in \mathbb{R}^{1\times 2(n-4)}$ is 1, whilst the remaining entries of C_p are zeros. Since $Y_n \approx Y_{n-2}$ for large enough n, the shear force from (6) can be approximated by

$$\begin{aligned} f(t) &\approx -\nu\frac{\partial Y_{n-2}}{\partial t} - \kappa Y_{n-2}\\ &= -\nu(x_{2n-8} + \frac{2I_{n-2}}{\rho A_{n-2}\delta\zeta I_n}\alpha f) - \kappa x_{2n-9} \end{aligned}\tag{23}$$

or

$$f(t) \approx -\left(\frac{1}{1 + \nu\alpha\frac{2I_{n-2}}{\rho A_{n-2}\delta\zeta I_n}}\right)(\nu x_{2n-8} + \kappa x_{2n-9})$$

Note that the κ and ν are unknown and vary with tip/specimen distance.

B. Sliding mode observer

With a large number of nodes, the model in (21) is a 'close' approximation to the real PDE – at the cost of significant computation. Since a high order system is not convenient for computation, particularly for on-line implementation (which is the ultimate goal of the project), a model

reduction technique will be employed to extract a lower order model. There is significant literature on this topic, and a broad range of model reduction methods are available in the literature. In this paper, we will use a standard balanced truncation method by Moore [30], which is available in Matlab. Hence, for observer design, a model of the form

$$\begin{aligned} \dot{x}(t) &= Ax(t) + Bu(t) + Df(t) && (24)\\ y(t) &= Cx(t) && (25) \end{aligned}$$

will be used where $x \in \mathbb{R}^{n_r}$ is the state vector of the reduced model, n_r is the order of the model, and A, B, C, D are fixed matrices of appropriate dimension obtained from the balanced truncation method.

With the above model, we can use a number of sliding mode observers to estimate the shear force $f(t)$ from knowledge of only $y(t)$ and $u(t)$. In the literature, numerous methods for designing sliding mode observers have appeared: see for example [22] and the references therein. In this paper, the design will be based on the observer proposed in [19] for square systems. The sliding mode observer employed here is given as follows:

$$\begin{aligned} \dot{\hat{x}}(t) &= A\hat{x}(t) + Bu(t) - Ge_y(t) + Dv && (26)\\ \hat{y}(t) &= C\hat{x}(t) && (27) \end{aligned}$$

where the output estimation error $e_y(t) = \hat{y}(t) - y(t)$ is driven to zero in finite time [31]. In (26) the gain G is chosen so that there exists a symmetric positive definite matrix P such that

$$P(A - GC) + (A - GC)^T P < 0 \qquad (28)$$

and

$$PD = (FC)^T \qquad (29)$$

for some $F \in \mathbb{R}$. This is essentially the observer initially proposed by Walcott & Zak [32]. The nonlinear injection signal in (26) is given by

$$v = \begin{cases} -\sigma \frac{Fe_y}{\|Fe_y\|} & \text{if } e_y \neq 0, \\ 0 & \text{otherwise} \end{cases} \qquad (30)$$

and the scalar σ must be chosen so that $\|f(t)\| \leq \sigma$. In order to design a feasible observer, of the structure in (26)-(30), the following must be satisfied [31], [33]:

- rank$(CD) = 1$ or in this case $CD \neq 0$
- invariant zeros of (A, D, C) must lie in $\mathbb{C}_-$

Here because the system is square, an analytic solution to the design problem can be employed. In this paper the approach proposed in [19] will be employed to synthesize the gain G. For the cantilever problem, despite the model reduction employed to create (A, D, C), the resulting state space is still relatively large, and more importantly badly numerically conditioned. The approach in [19] does not employ significant transformations of the state-space (compared to [31] for example) and this is advantageous here. The only transformation required is an orthogonal one to obtain 'regular form' for the pair (A, D) [31]. Thus there exists a linear orthogonal change of coordinates $x \mapsto Tx$ such that in the new coordinate system

$$\begin{aligned} \dot{x}_1(t) &= A_1x_1(t) + A_2x_2(t) + B_1u(t) && (31)\\ \dot{x}_2(t) &= A_3x_1(t) + A_4x_2(t) + B_2u(t) + D_2f(t) && (32)\\ y(t) &= C_1x_1(t) + C_2x_2(t) && (33) \end{aligned}$$

where the partitions $x_1 \in \mathbb{R}^{n_r-1}$, $x_2 \in \mathbb{R}$ and the matrix sub-blocks $A_1, \ldots, A_4$ have no special structure. In (32), $D_2 \neq 0$. As argued in [19], in the regular form coordinates, a suitable choice for the observer gain is

$$G = \begin{bmatrix} A_2C_2^{-1} \\ A_4C_2^{-1} - C_2^{-1}A_4^s \end{bmatrix} \qquad (34)$$

where A_4^s is a negative design scalar. For details see [19]. Note that $C_2 \neq 0$ since $CD = C_2D_2$ and $CD \neq 0$ by assumption. The scalar F from (30) satisfies

$$F = P_2C_2D_2 \qquad (35)$$

for some positive scalar P_2 (in this case).

The state estimation error col$(e_1, e_2) = x - \hat{x}$ satisfies

$$\begin{aligned} \dot{e}_1(t) &= (A_1 - A_2C_2^{-1}C_1)e_1(t) && (36)\\ \dot{e}_2(t) &= \tilde{A}_3e_1(t) + C_2^{-1}A_4^sC_2e_2(t) + D_2(f(t) - v) && (37) \end{aligned}$$

where $\tilde{A}_3 = A_3 - A_4C_2^{-1}C_1 - C_2A_4^sC_1$. During the sliding motion, $e_y = 0$ and $\dot{e}_y = 0$ [31] and therefore $e_2 = \dot{e}_2 = 0$ and from (37) it follows that

$$v_{eq} = f + D_2^{-1}\tilde{A}_3e_1(t) \qquad (38)$$

where v_{eq} is the so-called 'equivalent injection' necessary to maintain a sliding motion [31]. Since the eigenvalues of $(A_1 - A_2C_2^{-1}C_1)$ are the invariant zeros of (A, D, C), the subsystem (36) is by assumption a stable autonomous system and $e_1(t) \to 0$ as $t \to \infty$ and therefore

$$v_{eq} \to f(t) \qquad (39)$$

In practice the equivalent injection v_{eq} (and hence the shear force $f(t)$), can be extracted from (30) by using a low-pass filter. In our case, a first order low pass filter is used to obtain the force estimate the equivalent injection

$$\dot{\tilde{v}} = -k\tilde{v} + kv, \quad k > 0, \ \tilde{f}(0) = 0. \qquad (40)$$

and so for a large value of k, it follows that $\tilde{v} \approx v_{eq} \to f(t)$. Consequently using the sliding mode observer, changes in the shear force $f(t)$ can be estimated in real time as the tip descends towards the sample through the ordered water layers. However a more succinct indication of these changes can observed from the changes in the shear force model parameters κ and ν from (6). Here it is proposed that in addition to estimating $f(t)$ in real time, this information will be used to estimate $\kappa(t)$ and $\nu(t)$ from the model given in (6) via least squares [34]. In (6), the left hand side is available from the equivalent injection signal which is extracted from the nonlinear injection term in (30) via a low-pass filter (40). Consequently to obviate the effect of any phase lag

associated with the filter, all time dependent terms on the right hand side of (6) will also be subject to the same filter:

$$\dot{\tilde{Y}} = -k\tilde{Y} + kY(L),\ \tilde{Y}(0) = 0. \tag{41}$$

Then it follows from (6) that

$$\tilde{f}(t) = -\nu\frac{\partial\tilde{Y}}{\partial t} - \kappa\tilde{Y} \tag{42}$$

Furthermore, the filter in (41) enables us to reconstruct $\frac{\partial\tilde{Y}}{\partial t}$ as the right hand of (41), i.e. as $-k\tilde{Y} + kY$, and hence no measured knowledge of $\frac{\partial\tilde{Y}}{\partial t}$ is required (see for example [34]). Standard recursive least squares procedures can then be used to estimate κ and ν.

Remark 2.1: Note the amalgamation of sliding mode observers and least squares methods has appeared in the sliding mode literature: see for example [35]. Here the formulation is quite bespoke for the cantilever problem at hand and the observer state reconstructions do not provide sufficient information to deduce directly κ and ν. Consequently the use of the low-pass filters and the ideas of [34] facilitate the estimation of the shear force model parameters based only on the estimates of $f(t)$ and measurements of $Y(L)$.

III. Simulation Results

The cantilever is made of Silicon Nitride (Si3N4) and the parameters are given as follows: Young's modulus $E = 290Gpa$, density $\rho = 3185kg/m^3$, length $L = 26\mu m$, width $W = 2\mu m$, thickness $t_c = 200nm$ [15]. Hence, $A_s = Wt_c$ and $I = 1/12Wt_c^3$. The loss factor due to internal friction in the probe is $\alpha = 1.36655 \times 10^{-8}$ and the loss factor due to the water drag $\gamma = 100$. The elastic interaction and dissipative interaction constants are $\kappa = 1.02124$, $\nu = 5.38214 \times 10^{-6}$, and $\kappa = 0.070114$, $\nu = 3.962516 \times 10^{-7}$ corresponding to the tip-sample distances of $0.5nm$ and $1nm$ respectively. We have chosen a sinusoidal signal with amplitude $d_0 = 0.828nm$ and frequency $\omega = 28813rad/s$. Here, we use the same input signal and the same liquid environment as in [28].

For the simulations, we have chosen $n = 50$. Because of the high frequency of the excitation input signal, we need to observe the simulations at a small time scale. Therefore, for convenient simulation, the matrices A, B have been divided by 1000 which effectively implies a change in the time scale by a factor of 1000. Similarly, the input signal is scaled by multiplying by 1×10^9 so that it can be observed at the nanoscale level. The order of the reduced system is $n_r = 9$. The matrix A_4^s is chosen so that the user defined pole of the observer is -1×10^6. In this example, we have chosen $\sigma = 100$. The nonlinear injection signal v and the measured tip position $Y(L)$ are fed through identical low-pass filters (40)-(41) with $k = 2000$ to extract the equivalent injection v_{eq} and the filtered $\tilde{Y}(L)$ for the least squares calculations. The sliding mode observer designed from the previous section is connected to the 'real plant' of order 92. Both the full-order and reduced systems satisfy the conditions for sliding mode observer design discussed earlier. The initial condition of the state variables for the full-order model is zero and for the observer $[0, 0, 0, 0, 0, 0, 0, 0, 8 \times 10^{-3}nm]$. Simulations have been conducted in which the output $Y(L)$ is assumed to be measured perfectly, and also in the situation where it is corrupted by additive Gaussian noise. Practically this could be caused not only by sensor measurement noise, but also by Brownian/Thermal noise, which has significant effects on the real TDFM system. Two scenarios have been considered: one where the tip is assumed to be away from the specimen ($\kappa = 0.07$ and $\nu = 0.004$), and one where it is near to the specimen sample ($\kappa = 1.02$ and $\nu = 0.0004$). Figure 2 and Figure 5 show that the observer reconstructs the shear force with reasonable accuracy for the two different cantilever distances. The parameters κ and ν are estimated with good accuracy (Figs. 3, 4)).

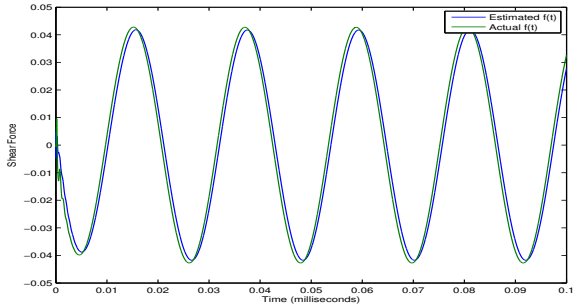

Fig. 2. The shear force and reconstruction signal for a tip-sample distance of $0.5nm$.

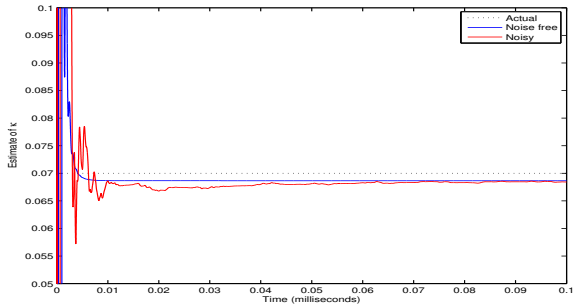

Fig. 3. Estimates of the shear force model parameter κ distance of $0.5nm$.

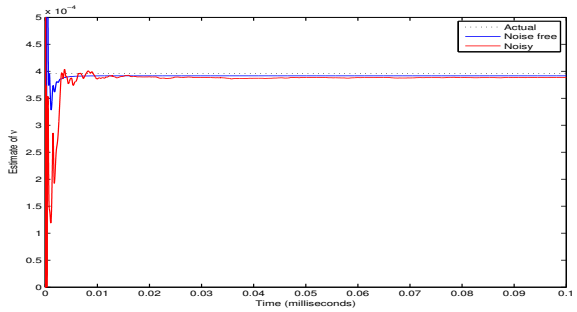

Fig. 4. Estimates of the shear force model parameter ν distance of $0.5nm$.

IV. Conclusion

It has been shown that it is possible to obtain a real time estimate of the shear forces affecting the VOC of a TDFM.

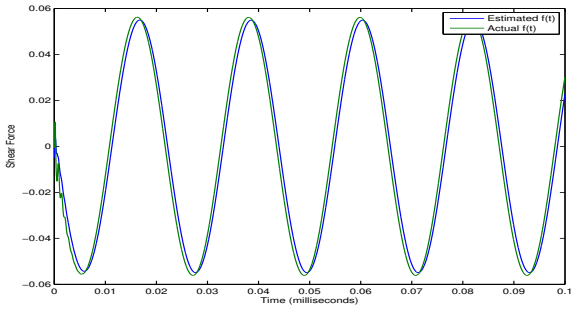

Fig. 5. The shear force and reconstruction signal for a tip-sample distance of $1nm$.

This has been complemented by a parametric representation of the shear force, in terms of elastic and dissipative constants, which gives a scaled measure of the cantilever-specimen distance. To estimate the shear force, it has been shown that it is sufficient to use a reduced order model (via balanced truncation), derived from an approximate ODE model of the cantilever dynamics. Simulations show that the sliding mode observer based on this reduced model, can reconstruct the unknown shear force with good accuracy even for measurement signals subject to noise. Future experiments will be carried out to validate our method on the TDFM rig at the Centre for NSQI at Bristol.

REFERENCES

[1] G. Binnig, C. Quate, and C. Gerber, "Atomic force microscope," *Physical Review Letters*, 1986.

[2] K. A. Ramirez-Aguilar and K. L. Rowlen, "Tip characterization from afm images of nanometric spherical particles," *Langmuir*, vol. 14, no. 9, pp. 2562–2566, 1998.

[3] R. Howland and L. Benatar, *Practical Guide to Scanning Probe Microscopy*. Park Scientific Instruments: Sunnyvale, CA, USA, 1993.

[4] T. Ando, T. Uchihashi, and T. Fukuma, "High-speed atomic force microscopy for nano-visualization of dynamic biomolecular processes," *Progress in Surface Science*, vol. 83, no. 79, pp. 337 – 437, 2008.

[5] T. Ando, "Control techniques in high-speed atomic force microscopy," in *American Control Conference, 2008*, june 2008, pp. 3194 –3200.

[6] S. Kuiper and G. Schitter, "Improving the imaging speed of afm with modern control techniques," in *Control Technologies for Emerging Micro and Nanoscale Systems*, ser. Lecture Notes in Control and Information Sciences, E. Eleftheriou and S. Moheimani, Eds. Springer Berlin / Heidelberg, 2011, vol. 413, pp. 83–100.

[7] G. Schitter, P. J. Thurner, and P. K. Hansma, "Design and input-shaping control of a novel scanner for high-speed atomic force microscopy," *Mechatronics*, vol. 18, no. 56, pp. 282 – 288, 2008.

[8] P. K. Hansma, G. Schitter, G. E. Fantner, and C. Prater, "High-speed atomic force microscopy," *Science*, vol. 314, no. 5799, pp. 601–602, 2006.

[9] G. E. Fantner, G. Schitter, J. H. Kindt, T. Ivanov, K. Ivanova, R. Patel, N. Holten-Andersen, J. Adams, P. J. Thurner, I. W. Rangelow, and P. K. Hansma, "Components for high speed atomic force microscopy," *Ultramicroscopy*, vol. 106, no. 8-9, pp. 881 – 887, 2006.

[10] M. Antognozzi, A. Humphris, and M. Miles, "Observation of molecular layering in a confined water film and study of the layers viscoelastic properties," *Applied Physics Letters*, vol. 78, no. 3, pp. 300–302, 2001.

[11] P. J. James, M. Antognozzi, J. Tamayo, T. J. McMaster, J. M. Newton, and M. J. Miles, "Interpretation of contrast in tapping mode afm and shear force microscopy. a study of nafion," *Langmuir*, vol. 17, no. 2, pp. 349–360, 2001.

[12] R. Brunner, O. Marti, and O. Hollricher, "Influence of environmental conditions on shearforce distance control in near-field optical microscopy," *Journal of Applied Physics*, vol. 86, no. 12, pp. 7100–7106, 1999.

[13] N. A. Burnham and R. J. Colton, "Measuring the nanomechanical properties and surface forces of materials using an atomic force microscope," *Journal of Vacuum Science Technology*, 1989.

[14] M. Antognozzi, A. Ulcinas, L. Picco, S. H. Simpson, P. J. Heard, M. D. Szczelkun, B. Brenner, and M. J. Miles, "A new detection system for extremely small vertically mounted cantilevers," *Nanotechnology*, vol. 19, no. 38, p. 384002, 2008.

[15] R. L. Harniman, J. A. Vicary, J. K. H. Hörber, L. M. Picco, M. J. Miles, and M. Antognozzi, "Methods for imaging dna in liquid with lateral molecular-force microscopy," *Nanotechnology*, vol. 23, no. 8, p. 085703, 2012.

[16] J. Vicary, A. Ulcinas, and J. H "Micro-fabricated mechanical sensors for lateral molecular-force microscopy," *Ultramicroscopy*, vol. 111, no. 11, pp. 1547 – 1552, 2011.

[17] G. Besancon, A. Voda, and M. Alma, "On observer-based estimation enhancement by parametric amplification in a weak force measurement device," in *Decision and Control, 2008. CDC 2008. 47th IEEE Conference on*, 2008, pp. 5200 –5205.

[18] X. Xu, J. Melcher, and A. Raman, "Accurate force spectroscopy in tapping mode atomic force microscopy in liquids," *Phys. Rev. B*, vol. 81, pp. 035 407–1–035 407–7, 2010.

[19] C. Edwards and S. K. Spurgeon, "Sliding mode output tracking with application to a multivariable high temperature furnace problem," *International Journal of Robust and Nonlinear Control*, vol. 7, no. 4, pp. 337–351, 1997.

[20] C. Tan and C. Edwards, "Sliding mode observers for reconstruction of simultaneous actuator and sensor faults," in *Proceedings of the Conference on Decision and Control, CDC '03, Hawaii*, 2003.

[21] L. Fridman, Y. Shtessel, C. Edwards, and X.-G. Yan, "Higher-order sliding-mode observer for state estimation and input reconstruction in nonlinear systems," *International Journal of Robust and Nonlinear Control*, vol. 18, no. 4-5, pp. 399–412, 2008.

[22] C. P. Tan and C. Edwards, "Robust fault reconstruction in uncertain linear systems using multiple sliding mode observers in cascade," *IEEE Transactions on Automatic Control*, vol. 55, no. 4, pp. 855 –867, 2010.

[23] L. Fridman, A. Levant, and J. Davila, "High-order sliding-mode observation and identification for linear systems with unknown inputs," in *Proceedings of the IEEE Conference on Decision and Control, San Diego, CA*, 2006, pp. 5567–5572.

[24] C. Edwards, S. K. Spurgeon, and R. J. Patton, "Sliding mode observers for fault detection and isolation," *Automatica*, vol. 36, no. 4, pp. 541 – 553, 2000.

[25] X.-G. Yan and C. Edwards, "Nonlinear robust fault reconstruction and estimation using a sliding mode observer," *Automatica*, vol. 43, no. 9, pp. 1605 – 1614, 2007.

[26] H. Alwi, C. Edwards, and C. P. Tan, "Sliding mode estimation schemes for incipient sensor faults," *Automatica*, vol. 45, no. 7, pp. 1679 – 1685, 2009.

[27] M. Antognozzi, D. Binger, A. Humphris, P. James, and M. Miles, "Modeling of cylindrically tapered cantilevers for transverse dynamic force microscopy (tdfm)," *Ultramicroscopy*, vol. 86, no. 1-2, pp. 223 – 232, 2001.

[28] M. Antognozzi, "Investigation of the shear force contrast mechanism in transverse dynamic force microscopy," Ph.D. dissertation, Univeristy of Bristol, 2000.

[29] W. E. Schiesser and G. W. Griffiths, *A Compendium of Partial Differential Equation Models: Method of Lines Analysis with Matlab*. Cambridge: Cambridge University Press, 2009.

[30] B. Moore, "Principal component analysis in linear systems: Controllability, observability, and model reduction," *IEEE Transactions on Automatic Control*, vol. 26, no. 1, pp. 17 – 32, 1981.

[31] C. Edwards and S. Spurgeon, *Sliding Mode Control: Theory and Applications*. Taylor & Francis, 1998.

[32] B. Walcott and S. Żak, "State observation of nonlinear uncertain dynamical systems," *IEEE Transaction on Automatic Control*, vol. 32, pp. 166–170, 1987.

[33] C. Edwards, X. Yan, and S. Spurgeon, "On the solvability of the constrained lyapunov problem," *IEEE Transactions Automatic Control*, vol. 52, pp. 1982–1987, 2007.

[34] S. Sastry and M. Bodson, *Adaptive Control: Stability, Convergence, and Robustness*. Prentice-Hall, 1994.

[35] S. Baev, I. Shkolnikov, Y. Shtessel, and A. Poznyak, "Sliding mode parameter identification of systems with measurement noise," *International Journal of Systems Science*, vol. 38, pp. 871–878, 2007.